NANO LETTERS

Letter

pubs.acs.org/NanoLett

Synthesis of Ultrathin Copper Nanowires Using Tris(trimethylsilyl)silane for High-Performance and Low-Haze Transparent Conductors

Fan Cui,[†,‡,§] Yi Yu,[†,§] Letian Dou,[†,‡,§] Jianwei Sun,[†,§] Qin Yang,[†] Christian Schildknecht,[‡] Kerstin Schierle-Arndt,[‡] and Peidong Yang*[,†,‡,§,∥,⊥]

[†]Department of Chemistry, University of California, Berkeley, California 94720, United States

[‡]California Research Alliance (CARA), BASF Corporation, Berkeley, California 94720, United States

[§]Materials Sciences Division, Lawrence Berkeley National Laboratory, Berkeley, California 94720, United States

[∥]Kavli Energy NanoSciences Institute at the University of California, Berkeley, and the Lawrence Berkeley National Laboratory, Berkeley, California 94720, United States

[⊥]Department of Materials Science and Engineering, University of California, Berkeley, California 94720, United States

Supporting Information

ABSTRACT: Colloidal metal nanowire based transparent conductors are excellent candidates to replace indium−tin−oxide (ITO) owing to their outstanding balance between transparency and conductivity, flexibility, and solution-processability. Copper stands out as a promising material candidate due to its high intrinsic conductivity and earth abundance. Here, we report a new synthetic approach, using tris(trimethylsilyl)silane as a mild reducing reagent, for synthesizing high-quality, ultrathin, and monodispersed copper nanowires, with an average diameter of 17.5 nm and a mean length of 17 μm. A study of the growth mechanism using high-resolution transmission electron microscopy reveals that the copper nanowires adopt a five-fold twinned structure and evolve from decahedral nanoseeds. Fabricated transparent conducting films exhibit excellent transparency and conductivity. An additional advantage of our nanowire transparent conductors is highlighted through reduced optical haze factors (forward light scattering) due to the small nanowire diameter.

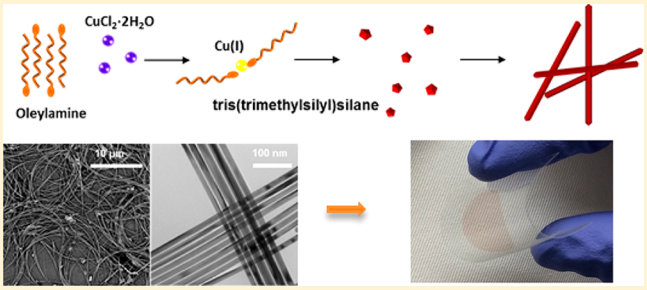

KEYWORDS: *Ultrathin copper nanowires, tris(trimethylsilyl)silane, growth mechanism, transparent conductor, reduced haze*

Transparent conductors are indispensable in consumer electronics, such as touch panels, displays, photovoltaic devices, and electrochromic windows.[1−4] The majority of current technologies rely on indium−tin−oxide (ITO)-based thin films, which have high optical transparency and low electrical resistivity.[5] However, ITO suffers from several drawbacks, including the high cost of sputtering manufacturing techniques,[6] low flexibility,[7] the scarcity of indium, and strong optical absorption in the near-infrared (NIR) wavelength window. A wide variety of materials, such as conducting polymers,[8] graphene,[9] carbon nanotubes (CNTs),[10] patterned metal gratings,[11] and metallic nanowire meshes,[12] have been explored in an attempt to replace ITO as a transparent conductor. Among these alternative materials, metal nanowire network is currently among the most promising avenue to replace ITO and has received growing attention over the years.[13−17] Copper is a promising candidate for nanowire-based electrodes as it has high intrinsic conductivity (only second to silver), and it is very abundant (1000 times more abundant than silver).[6] It has been well established through theoretical simulations and experiments that the transparency/conductivity performance of a metal nanowire mesh film is largely determined by the aspect ratio of nanowires (over 400 is desired).[18] To achieve high transparency and good conductivity, many works have been devoted toward synthesizing long copper nanowires with small diameter. One approach to making copper nanowires is via electrospinning/metal evaporation.[19] Copper nanowires can also be obtained via colloidal chemistry by reducing Cu ion/ion complex in the presence of capping ligands. Notably, large aspect ratio copper nanowires (with diameter ranging from 15 to 100 nm) were successfully synthesized using reducing agents such as glucose,[20,21] ascorbic acid,[22,23] hydrazine,[24−26] and even primary amines with assistance from high pressure (hydrothermal),[27] catalysts (Pt,[28] Ni^{2+}[29]), or choice of more active Cu precursor.[30] Using these Cu nanowires, thin films with good optical

Received: August 25, 2015
Revised: October 11, 2015
Published: October 23, 2015

DOI: 10.1021/acs.nanolett.5b03422
Nano Lett. 2015, 15, 7610−7615

transmittance and electric conductivity have been achieved. Another important, yet often overlooked parameter of transparent conductor is haze: a measure of the scattering of light by a material that is responsible for the reduction in contrast and sharpness of objects viewed through it. The large amount of forward scattering due to dense microstructures limits the commercial appeal of metal nanowire conducting films. According to simulations, with the same area coverage, the haze factor of a nanowire mesh film is approximately linear to nanowire diameter (for nanowire with diameter smaller than 100 nm).[31] Hence, the metal nanowires' diameter should be small (e.g., <20 nm) to keep light scattering (haze) at a minimum and to afford a good transparency/conductance trade-off, while at the same time not too thin to introduce stability issues during film fabrications.[32,33]

Here, we report a new synthetic approach for achieving ultrathin high-quality copper nanowires with average diameter of 17.5 nm and mean length of 17 μm. For the first time, a tris(trimethylsilyl)silane is introduced as a mild reducing reagent in the metallic nanostructure synthesis. The silane approach is simple and straightforward, and it opens up new opportunities for inorganic nanomaterial synthesis. The nanowire growth mechanism is investigated by high-resolution transmission electron microscopy (HRTEM) and selected area electron diffraction (SAED). Transparent conducting thin films were next fabricated with excellent uniformity on glass substrates. The resulting thin films show improved conductivity, optical transparency, and reduced haze in comparison with reports thus far.

Figure 1a presents the chemical reaction and optical photos before and after the synthesis. In our synthesis, oleylamine

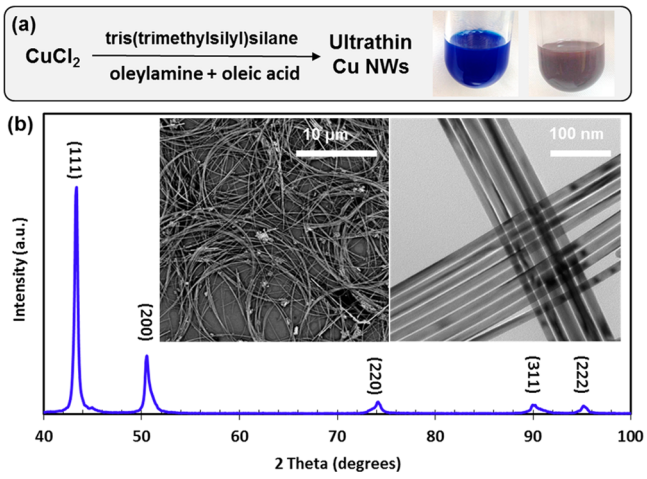

Figure 1. Synthesis of ultrathin copper nanowires. (a) Copper nanowire synthetic reaction and optical images of reactants (left inset) and products (right inset). (b) X-ray diffraction pattern of copper nanowires. Inset, SEM (left) and TEM (right) images of as-grown copper nanowires.

(OLA) is used as a coordinating ligand for the $CuCl_2$ precursor. During the reaction, the mixture forms Cu(II)−OLA complexes, which result in a clear blue solution. When the solution was placed under elevated temperature, Cu(II) species is gradually reduced to Cu(I) species at around 100 °C, which is indicated by a blue-to-light yellow color transition.[34] With further increase of temperature to about 165 °C, the clear yellow solution slowly turns reddish, which marks the formation of copper nanoparticles. Apart from being a coordinating solvent to copper precursors, OLA also serves as a capping ligand on the copper nanowire surface. Tris(trimethylsilyl)silane (TTMSS), which is widely used in organic synthesis, is introduced here as a mild reductant for the copper reduction, and it is found to play a key role for achieving high quality copper nanowires. Oleic acid serves as a supplementary ligand, to help enhance the copper nanowire dispersion and to prevent the wires from collapsing and aggregating at elevated temperatures (Figure S1). Figure 1b inset (left) shows the scanning electron microscopy (SEM) image of the ensemble copper product. The predominant products are nanowires (with less than 10% of nanoparticles by counts) with an average length measured to be 17 μm. The right inset is the transmission electron microscopy (TEM) image of the as-grown nanowires. The nanowires have a mean diameter of 17.5 nm with a standard deviation of ∼3 nm, which was calculated from 300 randomly selected images from different batches of the reaction. The X-ray diffraction (XRD) spectrum shown indicates that copper nanowires have a face-centered cubic (FCC) structure. The 2 theta peaks at 43.3°, 50.5°, 74.1°, 89.9°, and 95.1° correspond to the {111}, {200}, {220}, {311}, and {222} planes of the FCC copper.

The detailed structure of the copper nanowires was analyzed using HRTEM and SAED as shown in Figure 2a−d. Copper nanowires were shown to have 5-fold twinned pentagonal structure, which is commonly adopted by metal nanowires/nanorods materials.[15,35,36] The 5-fold symmetry of the as-grown copper nanowires can be visualized as consisting of five single-crystalline units (T1−T5) with a FCC structure, as illustrated in the insets of Figure 2a,c. Figure 2a,b shows HRTEM images and SAED patterns with the electron beam perpendicular to one of the side facets (indicated by red dot line). In Figure 2b, two sets of FCC pattern are observed: one along the zone axis [001] generated from the subunit T1 and the other in [1−1−2] direction generated from T3 and T4. The Moiré pattern in Figure 2a is generated from the overlap copper FCC unit cell {111} and {220} planes. When the electron beam is directed parallel to the side facets, as shown in Figure 2c,d, the diffraction pattern corresponds to the overlap of two FCC patterns with [1−10] and [−111] zone axes. A comprehensive analysis of the diffraction patterns and HRTEM images suggests that the nanowires have a five-fold symmetry with {100} facets as side surfaces and {111} planes bound at the ends. The growth direction is determined to proceed along [110] direction.

In an effort to better understand the one-dimensional growth mechanism, we investigated the product at the nucleation stage of the reaction. Figure 2e shows the reaction products after 2 h. The primary products are nanoparticles with a small number of elongated rods observed in the solution. A closer examination revealed that some of the nanoparticles are pentagonally shaped. The crystal structures of these nanoparticles were subsequently analyzed using HRTEM. Figure 2f shows the HRTEM image of one of the pentagonal dots, which exhibits a five-fold twinned structure. To further demonstrate the atomic details of the five twining and their twinning boundaries, a focal series of HRTEM images was utilized to reconstruct the exit-plane wave function in the middle area of the twin structure with optimized phase contrast. The result is shown with false color in the inset of Figure 2f, where perfect five subcrystal lattices together with sharp twin boundaries can be observed. Moreover, the 5-fold twin structure was confirmed by the FFT

DOI: 10.1021/acs.nanolett.5b03422
Nano Lett. 2015, 15, 7610−7615

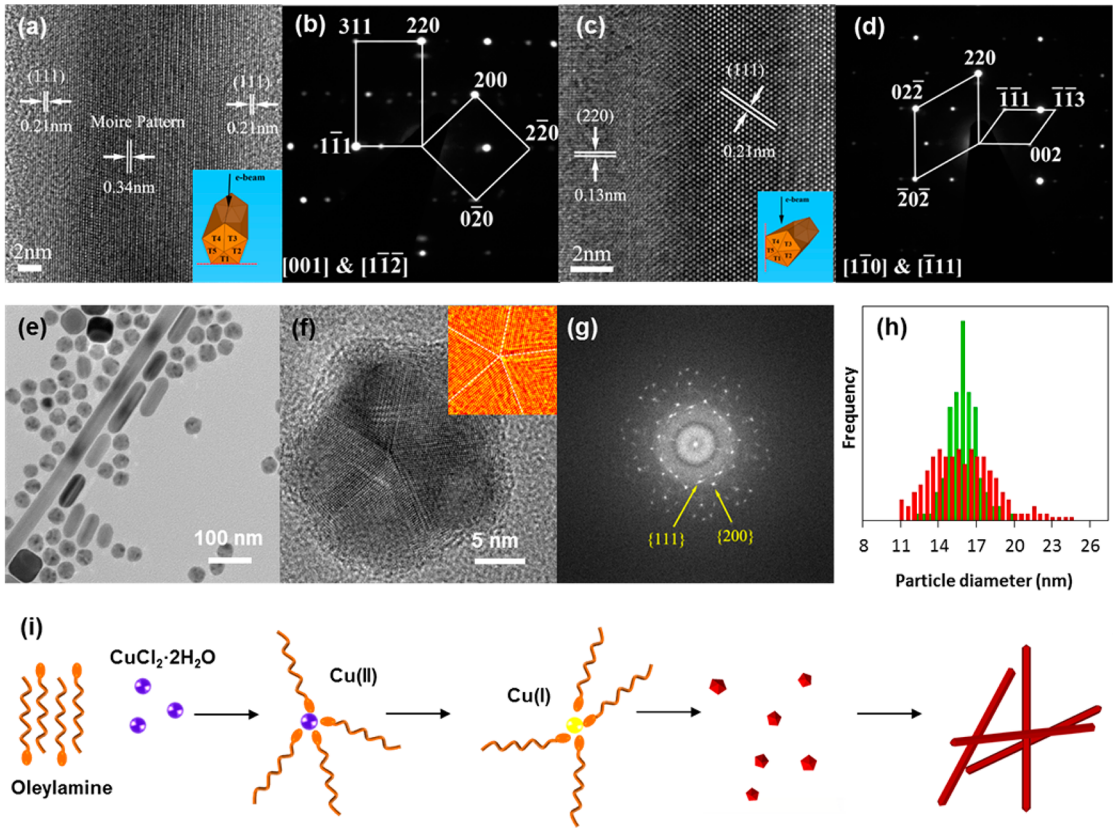

Figure 2. Atomic structure and growth mechanism of copper nanowires. (a) HRTEM images and (b) SAED pattern when one of the side surfaces is perpendicular to the electron beam as demonstrated in (a) inset. (c) HRTEM images and (d) SAED pattern when one of the side surfaces is parallel to the electron beam as demonstrated in (c) inset. (e) TEM images of Cu products when the reaction was carried out for 2 h. (f) HRTEM images and (g) fast Fourier transformation (FFT) pattern of five twinned decahedral nanoparticles. (h) Statistic and distribution of decahedral seeds diameter and final nanowire diameter (green: nanoparticles; red: nanowires). (i) Schematics of copper source reduction, five twined seeds nucleation, and nanowire evolution.

pattern of Figure 2f. The pattern (Figure 2g) gives an unambiguous representation of its five-fold symmetry. Note that nanoparticles with a square shape were also observed within this ensemble. These copper cubes were found to be single-crystalline (Figure S3). Given the five-twinned nature of the copper nanowires, the pentagonal and not the cubic nanoparticles were believed to be the starting seeds of the nanowires. To further confirm this hypothesis, a comparison between the diameters of the nanowires and the irregular dots was made (Figure 2h). The average diameter of the particles was measured to be 16.1 ± 1.2 nm based on 300 randomly selected dots in the TEM images. The diameter of the seeds has a strong correlation with that of the nanowires.

Figure 2i summarizes the proposed mechanism. A Cu(II) complex is initially converted to a Cu(I) species at 100 °C, then reduced further to Cu(0) at 150 °C via TTMSS. It is believed that TTMSS decomposes at over 150 °C with thermal cleavage of the Si−H bond. The silicon fragment can act as electron donor. It is relatively stable in the solution due to the protection of its bulky ligands and slowly reacts with the Cu(I) complex to produce Cu(0). Aside from acting solely as a reducing agent TTMSS plays a key role in forming ultrathin nanowires: the mild reducing power of TTMSS affords sufficiently slow reduction kinetics to allow time for the nucleation of the nanoseeds and subsequent nanowire growth. The nucleation favors multiply twinned decahedral seeds bounded by the more closely packed {111} planes. Twinning is often observed among FCC structured materials (particularly noble metal elements), with low twin boundary energy and surface energy difference.[37] The anisotropic elongation is modulated by OLA and a high concentration of amine is favorable to asymmetric growth (see SI, Figure S4). This can be explained by the fact that OLA preferentially binds with {100} over {111} planes.[38] Loosely packed {100} planes tend to offer more space for the attachment of bulky surfactants and copper complex. Moreover, the more closely packed {111} facets serve as low-surface energy sites for the deposition of Cu(0) species. The single-crystalline copper cubes, which nucleated before the five-twinned seeds, do not have a selected capping effect and thus do not serve as the seed toward anisotropic growth. These dots grow in size through Ostwald ripening during the reaction and account for undesired byproducts (Figure S5). The size of nanowires can be modified by changing reducing reagent amount and copper precursor concentration (see SI, Table S1). For example, nanowire diameter can be tuned from 15.5 to 22.5 nm when the molar ratio of TTMSS/$CuCl_2$ decreases from 8 to 2 (Figure S6).

Following synthesis, we next fabricated high-performance copper nanowire electrodes on glass using a filtration method. A dilute copper nanowire suspension was filtered through a nitrocellulose membrane through vacuum filtration, and the resulting film was subsequently transferred onto a glass substrate by pressing it against nitrocellulose membrane. Then, the electrode was annealed under forming gas (10%

DOI: 10.1021/acs.nanolett.5b03422
Nano Lett. 2015, 15, 7610−7615

hydrogen in argon) at around 200 °C to remove surface organic ligands and native oxides, and more importantly, to partially sinter the wires together to create intimate contact junctions (Figure S7). The heat treatment is found to have a considerable impact on the film properties. As shown in Figures S8 and S9, overheating easily breaks the copper nanowires due to their ultrathin diameters and consequently depressed melting points, while under-heating does not provide enough thermal energy to weld the individual nanowires together.

Figure 3a shows the optical images of the copper nanowire transparent conductor with different loading amounts. Figure 3b shows their corresponding SEM images, transmittance spectra, and measured sheet resistances. The films show great transparency from ultraviolet−visible range to infrared (350−1700 nm), rendering them suitable materials not only for displays in consumer electronics but also for photovoltaic cells or thermal applications, where transmission in the near-infrared region is also important. Moreover, the conducting films exhibit outstanding performance in the trade-off between transparency and resistance as plotted in Figure 3c. For a film with transmittance of 77%, the sheet resistance is as low as 5.32 ohms/sq. As the transmittance increases to 86%, the sheet resistance increases slightly to 15.0 ohms/sq. Another sample shows 90% in transmittance and 34.8 ohms/sq in sheet resistance. This performance clearly stands out in comparison with other reports on solution-based copper nanowire/nanofiber transparent conductors that demonstrate 50 ohms/sq at 90%,[19] 75 ohms/sq at 88%,[26] 35 ohms/sq at 85%,[28] and 23.3 ohms/sq at 78%.[29] Copper nanowire conducting films can also be fabricated on plastic substrates (Figure S10) via a modified processing approach. The nanowire film on PET shows great flexibility, and the sheet resistance is maintained at its original level after 1000 times bending cycles with bending radius as small as 2 mm (see Figure S11).

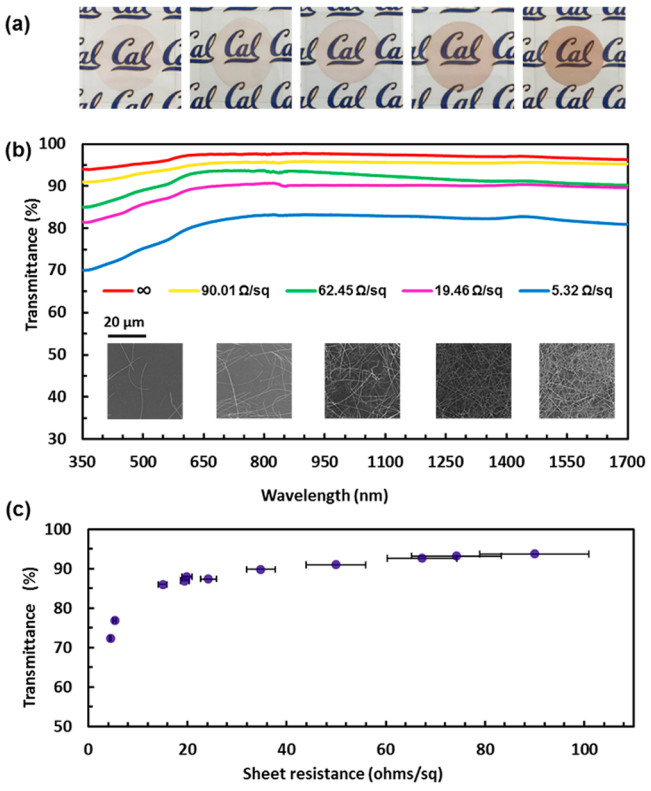

Figure 3. Ultrathin copper nanowire transparent conductor and its optical and electrical performance. (a) Optical images of transparent electrodes with increasing copper nanowire loading amounts (from left to right). (b) Wavelength-dependent transmittance, sheet resistance, and corresponding SEM images of transparent conductors. Substrate contribution is excluded. (c) Plot of transmittance versus conducting film sheet resistance. Characteristic transmittance data are acquired at 550 nm of wavelength.

The excellent performance of our copper nanowire electrodes can be attributed to several factors. First, the thin diameter of the nanowires would, in principle, boost light transmission while maintaining high conductance.[32] In addition, the well-controlled synthesis in this report results in high-quality, monodispersed copper nanowires. Oversized cluster byproducts, which greatly reduce transparency while contributing little to conductance, are minimized. Finally, the film fabrication process is carefully optimized to provide the best quality. Undesirable byproducts of the synthesis are mostly nanoparticles with the diameters between 30 and 100 nm (Figure S5). The 220 nm pore size nitrocellulose membrane used in the process enables the byproduct nanoparticles to be effectively washed through rather than be incorporated into the film (see Figure S12). Diluting the nanowire suspension as well as multiple rinses before and after the filtration also helps get rid of the undesired nanoparticles. The copper films also exhibit good stability in air over time. Typically, after the first 24 h of exposure in air, the conductivity shows a sharp decrease of about 30% and then stabilizes for up to 3 weeks tested (Figure S13).

Besides the merits of sheet resistance and transmission, optical haze is also an important factor in characterizing the quality of a transparent electrode. Haze is especially important in display applications where scattering will reduce the sharpness of an image. Haze is numerically defined as the percentage of transmitted light that is scattered more than a certain angle off the principal axis of the incident beam. In our case, the measurement follows the D1003-13 standard (see SI for detailed method). Large value in haze is an ongoing challenge for nanowire-based transparent electrodes because the nanowires are strong scattering centers. For example, Hu et al. reported a silver nanowire mesh with a scattering of 13% at 79% total transmittance, which means roughly 16.4% of transmitted light is scattered away off its original direction.[16] In another example, the forward light scattering of a copper fiber-based electrode contributed 10% of its 92% of total transmittance.[19] Even though some films show great conductivity with high transparency, a large portion of the transmitted light diverges from its original path, which makes them unsuitable in display applications.

The haze factor of a transparent conducting film heavily depends on nanowire diameter, with lower diameter nanowires featuring less haze.[31] We examined the haze of the thin films fabricated using our ultrathin copper nanowires. Figure 4a shows specular transmittance, diffuse transmittance, reflectance, and absorbance of a typical copper nanowire film with sheet resistance of 35 ohms/sq. When the light is directed at the copper film, 1.1% is reflected, 88.7% is transmitted, and 10.2% is absorbed. Of the total transmitted light, 86.1% is specular transmittance (direct transmission) and 2.6% is scattered away. Figure 4b lists several haze values at different total transmittance values. The haze value decreases almost linearly with the increase of total transmittance. When the total transmittance is 90%, the haze factor is only about 2−3%. The haze

DOI: 10.1021/acs.nanolett.5b03422
Nano Lett. 2015, 15, 7610−7615

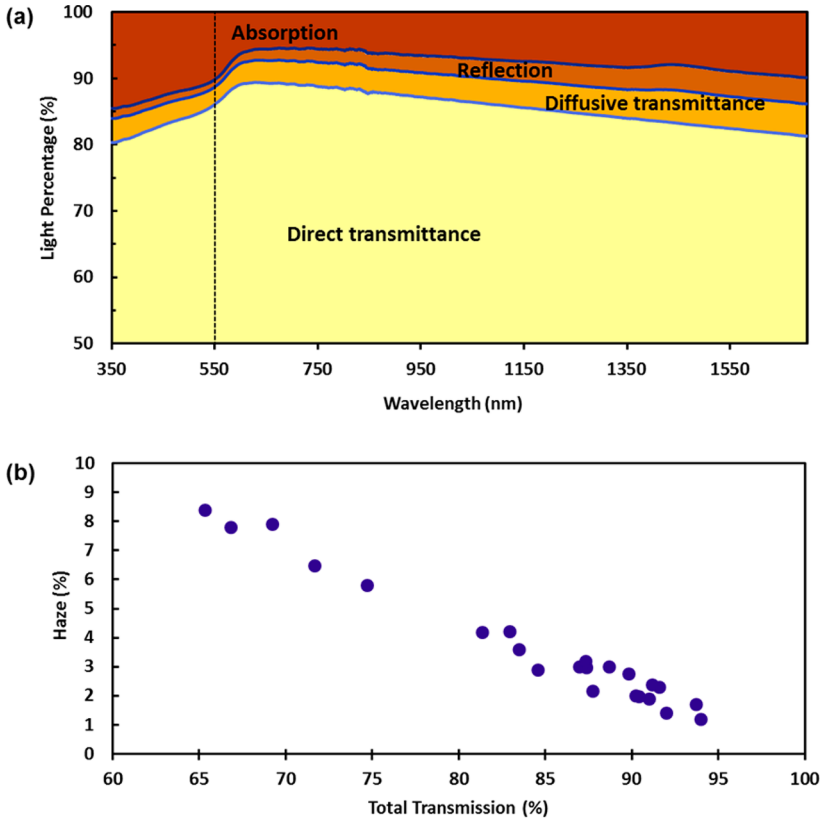

Figure 4. Light pathway through the copper film and haze factors. (a) Percentages of light absorbed, reflected, scattered (diffusive transmittance), and directly transmitted by a copper nanowire film. (b) Plot of the haze factors of copper nanowire conductors versus their total transmittance values. All characteristic optical property data are discussed at wavelength of 550 nm.

factor increases to 4% when the total transmittance is 81%. These results demonstrate that the ultrathin copper nanowire-based films show significantly lower scattering effect than that of similar nanowire transparent conductors reported in literatures. A direct comparison of the image sharpness behind a regular silver nanowire-based film and the ultrathin copper nanowire-based film with the same total transmittance is shown in Figure S15. The background pattern viewed through the silver film (made from nanowires with mean diameter of 50 nm) is visually more blurry.

In summary, we develop a novel synthetic approach using TTMSS as a mild reducing reagent to achieve ultrathin, uniform, and high-quality copper nanowires. This solution-based method is easily scalable and produces five-fold copper nanowires with diameter of 17.5 ± 3 nm. Detailed mechanism analysis of the growth is carried out to suggest that five-twinned pentagonal nanoparticles are ascertained to serve as seeds for the nanowire growth. High performance transparent conducting films were fabricated and exhibit high transparency with low sheet resistance. Furthermore, the resulting thin films show a dramatically reduced haze factor due to the ultrathin diameter, making them suitable for display applications. This work also demonstrates that TTMSS is a unique reducing reagent for metal nanomaterial synthesis, and our approach advances research into the commercialization of copper nanowire mesh electrodes.

■ ASSOCIATED CONTENT

Supporting Information

The Supporting Information is available free of charge on the ACS Publications website at DOI: 10.1021/acs.nanolett.5b03422.

Experimental details and additional figures (PDF)

■ AUTHOR INFORMATION

Corresponding Author

*E-mail: p_yang@berkeley.edu.

Notes

The authors declare no competing financial interest.

■ ACKNOWLEDGMENTS

This work was financially supported by BASF Corporation (Funding 20131459). We thank Dr. Sam Eaton, Mr. Nick Kornienko, and Dr. Anthony Fu for proofreading the manuscript. Work at the NCEM, Molecular Foundry was supported by the Office of Science, Office of Basic Energy Sciences, of the U.S. Department of Energy under Contract No. DE-AC02-05CH11231.

■ REFERENCES

(1) Tak, Y.; Kim, K.; Park, H.; Lee, K. *Thin Solid Films* **2002**, *411*, 12−16.
(2) Granqvist, C. G. *Sol. Energy Mater. Sol. Cells* **2007**, *91*, 1529−1598.
(3) Rauh, R. D. *Electrochim. Acta* **1999**, *44*, 3165−3176.
(4) Hecht, D. S.; Hu, L.; Irvin, G. *Adv. Mater.* **2011**, *23*, 1482−1513.
(5) Granqvist, C. G.; Hultaker, A. *Thin Solid Films* **2002**, *411*, 1−5.

DOI: 10.1021/acs.nanolett.5b03422
Nano Lett. 2015, 15, 7610−7615

(6) Ye, S.; Rathmell, A. R.; Chen, Z.; Stewart, I. E.; Wiley, B. J. *Adv. Mater.* **2014**, *26*, 6670−6687.
(7) Chen, Z.; Cotterell, B.; Wang, W.; Guenther, E.; Chua, S. A. *Thin Solid Films* **2001**, *394*, 201−205.
(8) Na, S. I.; Kim, S. S.; Jo, J.; Kim, D. Y. *Adv. Mater.* **2008**, *20*, 4061−4067.
(9) Bae, S.; Kim, H.; Lee, Y.; Xu, X.; Park, S.; Zheng, Y.; Balakrishnan, Y.; Tian, L.; Kim, H. R.; Song, Y. I.; et al. *Nat. Nanotechnol.* **2010**, *5*, 574−578.
(10) Wu, Z.; Chen, Z.; Du, X.; Logan, J. M.; Sippel, J.; Nikolou, M.; Kamaras, K.; Reynolds, J. R.; Tanner, D. B.; Hebard, A. F.; Rinzler, A. G. *Science* **2004**, *305*, 1273.
(11) Kang, M. G.; Guo, L. J. *Adv. Mater.* **2007**, *19*, 1391−1396.
(12) De, S.; Higgins, T. M.; Lyons, P. E.; Doherty, E. M.; Nirmalraj, P. N.; Blau, W. J.; Boland, J. J.; Coleman, J. N. *ACS Nano* **2009**, *3*, 1767−1774.
(13) Gaynor, W.; Burkhard, G. F.; McGehee, M. D.; Peumans, P. *Adv. Mater.* **2011**, *23*, 2905−2910.
(14) Zhu, R.; Chung, C.-H.; Cha, K. C.; Yang, W.; Zheng, Y. B.; Zhou, H.; Song, T.-B.; Chen, C.-C.; Weiss, P. S.; Li, G.; Yang, Y. *ACS Nano* **2011**, *5*, 9877−9882.
(15) Sun, Y.; Gates, B.; Mayers, B.; Xia, Y. *Nano Lett.* **2002**, *2*, 165−168.
(16) Hu, L.; Kim, H. S.; Lee, J.; Peumans, P.; Cui, Y. *ACS Nano* **2010**, *4*, 2955−2963.
(17) Song, M.; You, D. S.; Lim, K.; Park, S.; Jung, S.; Kim, C. S.; Kim, D.-H.; Kim, D.-G.; Kim, J.-K.; Park, J.; Kang, Y.-C.; Heo, J.; Jin, S.-H.; Park, J. H.; Kang, J.-W. *Adv. Funct. Mater.* **2013**, *23*, 4177−4184.
(18) Mutiso, R. M.; Sherrott, M. C.; Rathmell, A. R.; Wiley, B. J.; Winey, K. *ACS Nano* **2013**, *7*, 7654−7663.
(19) Wu, H.; Hu, L.; Rowell, M. W.; Kong, D.; Cha, J. J.; McDonough, J. R.; Cui, Y. *Nano Lett.* **2010**, *10*, 4242−4248.
(20) Mohl, M.; Pusztai, P.; Kukovecz, A.; Konya, Z. *Langmuir* **2010**, *26*, 16496−16502.
(21) Jin, M.; He, G.; Zhang, H.; Zeng, J.; Xie, Z.; Xia, Y. *Angew. Chem., Int. Ed.* **2011**, *50*, 10560−10564.
(22) Zhang, X.; Zhang, D.; Ni, X.; Zheng, H. *Solid State Commun.* **2006**, *139*, 412−414.
(23) Wang, W.; Li, G.; Zhang, Z. *J. Cryst. Growth* **2007**, *299*, 158−164.
(24) Chang, Y.; Lye, M.; Zeng, H. *Langmuir* **2005**, *21*, 3746−3748.
(25) Rathmell, A. R.; Wiley, B. J. *Adv. Mater.* **2011**, *23*, 4798−4803.
(26) Meng, F.; Jin, S. *Nano Lett.* **2012**, *12*, 234−239.
(27) Shi, Y.; Li, H.; Chen, L.; Huang, X. *Sci. Technol. Adv. Mater.* **2005**, *6*, 761−765.
(28) Zhang, D.; Wang, R.; Wen, M.; Weng, D.; Cui, X.; Sun, J.; Li, H.; Lu, Y. *J. Am. Chem. Soc.* **2012**, *134*, 14283−14286.
(29) Guo, H.; Lin, N.; Chen, Y.; Wang, Z.; Xie, Q.; Zheng, T.; Gao, N.; Li, S.; Kang, J.; Cai, D.; Peng, D. *Sci. Rep.* **2013**, *3*, 2323.
(30) Ye, E.; Zhang, S.; Liu, S.; Han, M. *Chem. - Eur. J.* **2011**, *17*, 3074−3077.
(31) Khanarian, G.; Joo, J.; Liu, X.-Q.; Eastman, P.; Werner, D.; O'Connell, K.; Trefonas, P. *J. Appl. Phys.* **2013**, *114*, 024302.
(32) Preston, C.; Xu, Y.; Han, X.; Munday, J. N.; Hu, L. *Nano Res.* **2013**, *6*, 461−468.
(33) Catrysse, P. B.; Fan, S. H. *Nano Lett.* **2010**, *10*, 2944−2949.
(34) Giuffrida, S.; Condorelli, G.; Costanzo, L.; Fragala, I.; Ventimiglia, G.; Vecchio, G. *Chem. Mater.* **2004**, *16*, 1260−1266.
(35) Kim, C.; Gu, W. H.; Briceno, M.; Robertson, I. M.; Choi, H.; Kim, K. *Adv. Mater.* **2008**, *20*, 1859−1863.
(36) Huang, X.; Zheng, N. *J. Am. Chem. Soc.* **2009**, *131*, 4602−4603.
(37) Hofmeister, H. *Encyclopedia of Nanoscience and Nanotechnology V.3*; Nalwa, H. S., Ed.; American Scientific Publishers: Los Angeles, CA, 2004.
(38) Johnson, C. J.; Dujardin, E.; Davis, S. A.; Murphy, C. J.; Mann, S. *J. Mater. Chem.* **2002**, *12*, 1765−1770.

DOI: 10.1021/acs.nanolett.5b03422
Nano Lett. 2015, 15, 7610−7615